Published in final edited form as:
Clin Cancer Res. 2011 April 15; 17(8): 2339–2349. doi:10.1158/1078-0432.CCR-10-2949.

Vorinostat increases expression of functional norepinephrine transporter in neuroblastoma *in vitro* and *in vivo* model systems

Swati S. More[1], **Melissa Itsara**[2], **Xiaodong Yang**[3], **Ethan G. Geier**[1], **Michelle K. Tadano**[1], **Youngho Seo**[4], **Henry F. VanBrocklin**[4], **William A. Weiss**[2], **Sabine Mueller**[2], **Daphne A. Haas-Kogan**[3], **Steven G. DuBois**[3], **Katherine K. Matthay**[3], and **Kathleen M. Giacomini**[1]

[1]Department of Bioengineering and Therapeutic Sciences, University of California, San Francisco, San Francisco, California 94143-0449

[2]Department of Neurology, University of California, San Francisco, San Francisco, California 94143-0449

[3]Department of Pediatrics, UCSF School of Medicine and UCSF Benioff Children's Hospital, University of California, San Francisco, San Francisco, California 94143-0449

[4]Department of Radiology and Biomedical Imaging, Center for Molecular and Functional Imaging, University of California, San Francisco, San Francisco, California 94143-0449

Abstract

Purpose—Histone deacetylase (HDAC) inhibition causes transcriptional activation or repression of several genes that in turn can influence the biodistribution of other chemotherapeutic agents. Here, we hypothesize that the combination of vorinostat, a HDAC inhibitor, with ^{131}I-metaiodobenzylguanidine (MIBG) would lead to preferential accumulation of the latter in neuroblastoma (NB) tumors via increased expression of the human norepinephrine transporter (NET).

Experimental Design—*In vitro* and *in vivo* experiments examined the effect of vorinostat on the expression of NET, an uptake transporter for ^{131}I-MIBG. Human NB cell lines (Kelly and SH-SY-5Y) and NB1691luc mouse xenografts were employed. The upregulated NET protein was characterized for its effect on ^{123}I-MIBG biodistribution.

Results—Preincubation of NB cell lines, Kelly and SH-SY-5Y, with vorinostat caused dose-dependent increases in NET mRNA and protein levels. Accompanying this was a corresponding dose-dependent increase in MIBG uptake in NB cell lines. Four-fold and 2.5 fold increases were observed in Kelly and SH-SY-5Y cells, respectively, pre-treated with vorinostat in comparison to untreated cells. Similarly, NB xenografts, created by intravenous tail vein injection of NB1691-luc, and harvested from nude mice livers treated with vorinostat (150 mg/kg i.p.) showed substantial increases in NET protein expression. Maximal effect of vorinostat pretreatment in NB xenografts on ^{123}I-MIBG biodistribution was observed in tumors that exhibited enhanced uptake in vorinostat treated (0.062 ± 0.011 μCi/(mg tissue-dose injected)) versus untreated mice (0.022 ± 0.003 μCi/(mg tissue-dose injected); $p < 0.05$).

Conclusions—The results of our study provide preclinical evidence that vorinostat treatment can enhance NB therapy with ^{131}I-MIBG.

Corresponding author: Professor KM Giacomini, Department of Bioengineering and Therapeutic Sciences, University of California at San Francisco, 1550 4th Street, San Francisco, CA 94158, USA. kathy.giacomini@ucsf.edu .

Keywords

norepinephrine transporter; MIBG; Vorinostat; histone deacetylase inhibitor; neuroblastoma xenograft; biodistribution

Introduction

Neuroblastoma (NB) is the most common extracranial solid tumor of childhood and is often diagnosed after metastasis has commenced.[1] Originating from primitive sympathetic ganglion cells, NB can arise at any site in the sympathetic nervous system, with the adrenal gland being the most common site of origin. About 50% of all NB patients are classified as "high-risk", with survival rates frequently being less than 40% with existing therapies.[2] Patients with high-risk disease are at significant risk for resistance to initial therapy and have a high incidence of relapse subsequent to successful chemo- or radio-therapy.[3] The unfavorable outcome for patients with relapsed or refractory disease creates an enormous need for novel therapeutic strategies with particularly high therapeutic indices for these patients.

As a sympathetic-derived tumor, NB cells typically possess capabilities of monoamine uptake, decarboxylation pathways for monoamine synthesis and monoamine secretion.[4] Of particular diagnostic and therapeutic value is the expression of the norepinephrine transporter (NET).[5] NET serves as an important uptake protein for the norepinephrine analog, meta-iodobenzylguanidine (MIBG), an agent used for the diagnosis and treatment of NB. The use of low-dose radiolabeled MIBG (typically ^{123}I-MIBG) enables imaging to identify the sites and extent of neuroblastoma spread.[6,7] The use of high-dose radiolabeled MIBG (^{131}I-MIBG) enables targeted radiotherapy for patients with neuroblastoma. Single agent studies have shown that ^{131}I-MIBG is one of the most active agents for the treatment of patients with relapsed or refractory neuroblastoma.[8] The use of ^{131}I-MIBG in NB is predicated on the concept that the radionuclide will selectively target NET expressing tumors and metastases and will not harm normal tissues, particularly those expressing NET. A strategy built upon this concept would fundamentally carry the potential to deliver the high therapeutic index needed for successful NB treatment. The aims of the current study consisted of 1) mapping of NET in various tissues 2) chemical induction of NET expression and 3) study of ^{131}I-MIBG uptake into tissues under the influence of a chemical NET expression modulator. The working hypothesis was that a chemical entity that results in enhanced expression of NET in NB cells would increase the concentration of ^{131}I-MIBG in those sites and lead to preferential radiotherapy. Tissues that do not express NET could be expected to resist damage by ^{131}I-MIBG.

One of the possible avenues of influencing the expression levels of NET was the inhibition of histone deacetylation by an agent like vorinostat (suberoylanilide hydroxamic acid, SAHA). Histone deacetylase (HDAC) inhibition in turn could be expected to cause generalized perturbation of cellular protein expression, possibly affecting NET expression. In this paper, we describe the results of proof-of-concept *in vitro* and *in vivo* experiments in human NB cell lines and NB xenografts. The results support our hypothesis, and have enabled us to obtain approval for the initiation of clinical trials that examine a combination therapy of vorinostat and ^{131}I-MIBG for the treatment of neuroblastoma [NANT N2007-03].

Materials and Methods

Drugs and Reagents

Radiolabeled ^{123}I-MIBG was purchased from GE Healthcare (Sunnyvale, CA, USA). Radiolabeled ^{3}H-norepinephrine was purchased from Perkin Elmer Life Sciences (Waltham, MA, USA). All other chemicals were purchased from Sigma (St. Louis, MO, USA). Vorinostat was synthesized in our laboratory using a combination of previously published methods.[9,10] All the experiments described herein were also conducted utilizing a clinical grade sample of vorinostat obtained from Merck for comparison purposes. Antibodies for Western blotting were obtained from the following sources: rat polyclonal anti-NET antibody from Alpha Diagnostic International (NET11-A; San Antonio, TX, USA), horseradish peroxidase-conjugated anti-rabbit (sc-2004; Santa Cruz) immunoglobulin was used as the secondary antibody and mouse monoclonal anti-β-actin antibody from Santa Cruz Biotechnology (Santa Cruz, CA). Lipofectamine 2000 and hygromycin B were from Invitrogen (Carlsbad, CA). The cell culture media DMEM H-21, RPMI 1640, and fetal bovine serum (FBS) were obtained from the Cell Culture Facility of the University of California, San Francisco (San Francisco, CA).

Cell Lines and Transfection

Cell lines stably transfected with human NET, HEK-hNET and empty vector, HEK-EV, were established by transfection of pcDNA5/FRT vector (Invitrogen) containing the full-length hNET cDNA and pcDNA5/FRT vector alone, respectively, into human embryonic kidney 293 (HEK293) Flp-In cells using LipofectAMINE 2000 (Invitrogen) as per manufacturer's instructions. The stable clones were selected with 75 μg/mL hygromycin B. All the NB cell lines (LAN5, SHEP, SH-SY-5Y, Kelly, SK-N-SH, SK-N-MC, NB1691 and NB1691-luc) used in the present study were obtained from the UCSF Cell Culture Facility.

Cell Culture

Stably transfected HEK293 cells were maintained in DMEM H-21 medium supplemented with 10% FBS, 100 units/mL penicillin and 100 units/mL streptomycin and 75 μg/mL hygromycin B. The culture medium for all the NB cell lines was RPMI 1640 containing 15% FBS, 1% MEM non-essential amino acids, 100 units/mL penicillin, and 100 μg/mL streptomycin. All cell lines were grown at 37°C in a humidified atmosphere with 5% CO_2/95% air.

Cellular Uptake of ^{3}H-NE or ^{123}I-MIBG

HEK-hNET cells were seeded in 24 well poly-D-lysine coated cell culture plates (BD Biosciences) in standard cell culture media and the uptake studies were conducted 24 hours after cell seeding. Cells were incubated in PBS buffer containing 15 nM ^{3}H-NE in the presence or absence of a NET specific inhibitor, desipramine (10 μM), at 37°C for 3 minutes. After 3 minutes, uptake was terminated by rapid removal of the buffer containing the compounds and three quick washings with ice-cold PBS buffer. The cells were lysed with 1 mL of 0.1% SDS/0.1 N NaOH solution for about one hour and the intracellular levels of radioactive NE were determined using liquid scintillation counting. Intracellular concentrations of norepinephrine were normalized to the total protein in each well using bicinchoninic acid (BCA) protein assay (Pierce, Rockford, IL).

The same procedure was followed for determination of ^{3}H-NE or ^{123}I-MIBG uptake rate in NB cell lines, SH-SY-5Y and Kelly. In this case, cells were exposed to increasing concentrations of vorinostat ranging from 0 to 5 μM for 24 h, followed by exposure to ^{3}H-NE or ^{123}I-MIBG in PBS buffer, at 37°C for 3 min. The intracellular levels of radioactivity corresponding to ^{3}H-NE were determined as described earlier and were normalized to the

total protein content in each well using BCA protein assay. The total concentration of ^{123}I-MIBG was measured in an automated Wallac 1480 Wizard gamma counter using the program RiaCalc Wiz (Wallac Oy; Turku, Finland). .

RNA Isolation

Total RNA was isolated from each of the NB cell line on 6-well plates using the Invitrogen Micro-to-Midi Total RNA Purification System according to the manufacturer's protocol. Extracted RNA was stored at −80 °C until use. Similarly, total RNA was isolated from 13 NB tumor samples. Samples of NB tumors were obtained from the UCSF Pediatric Solid Tumor Tissue Bank following procedures approved by the UCSF Committee on Human Research. Four samples were collected at initial diagnosis, eight samples were collected after the initiation of therapy, and the timing of sample collection was unknown for one sample. Five of the tumor samples were from initial diagnosis (no prior treatment). All of the other samples were from patients who had received some type of therapy.

Reverse transcriptase-polymerase chain reaction

Reverse transcription (RT) PCR of RNA samples was carried out with Superscript III (Invitrogen) using oligo$(dT)_{20}$ primers. Two microliters of RT reaction product was used for subsequent PCR (Taq DNA Polymerase, Invitrogen) consisting of 35 cycles with the following parameters: 94 °C for 30 s, 60 °C for 45 s, 72 °C for 1 min, followed by a final extension of 72 °C for 10 min and storage at 4 °C. Primers were designed to amplify a unique sequence of human NET (SLC6A2), each spanning intron–exon boundaries to ensure no genomic DNA was amplified. The PCR primers that were used for human: NET (Genbank accession number NM_001043) forward— ATTCTTCAAAGGCGTTGGCTAT and reverse— CAGGACACCACGCTCATAAA were designed to amplify a 262-bp fragment. Analysis of each PCR sample was then performed on 2% agarose gels containing 0.5 μg/ml ethidium bromide. Gels were visualized using a digital camera and image processing system (Kodak, Rochester NY, USA). RT-PCR analysis for GAPDH gene was used as an internal control for each sample.

Quantitative Real-Time PCR

For qRT-PCR analysis, 2 μg of total RNA isolated from NB cells and tumor samples were reverse transcribed using High Capacity cDNA Reverse Transcription Kit (Applied Biosytems, CA, USA) in a 20 μL volume reaction according to the manufacturer's protocol. The resulting cDNA was used as template for quantitative real-time PCR using TaqMan® Gene Expression Assays for human transporter NET (Assay ID: Hs00426573_m1*) and human GAPDH (Assay ID: Hs99999905_m1). Quantitative real-time PCR reaction was carried out in 96-well reaction plates in a volume of 10 μL using the Taqman® Fast Universal Master Mix (Applied Biosystems, Foster City, CA). Reactions were run on the Applied Biosystems 7500 Fast Real-Time PCR System with the following profile: 95 °C for 20 seconds followed by 40 cycles of 95 °C for 3 seconds and 60 °C for 30 seconds. The relative expression of each mRNA was calculated by the comparative method (ΔΔCt method). Firstly, the ΔCt value for each sample was obtained by subtracting the Ct value of GAPDH mRNA from the Ct value of the NET mRNA. Then the ΔΔCt value for each sample was obtained by subtracting the ΔCt value of another endogenous control, PGK1, from the ΔCt value of each sample. The mRNA expression level of NET was reported as the percentage of the expression of PGK1 calculated using the arithmetic formula $2^{-\Delta\Delta Ct}$ (ABI PRISM 7700 Sequence Detection system User Bulletin No. 2, P/N 4303859) multiplied by 100.

Western blot analysis

The total protein extracts from transfected HEK 293, NB cells and tumor samples were prepared using CellLytic M cell lysis buffer (Sigma) containing protease inhibitor cocktail at 4 °C for 10 min. The cell homogenate was spun for 10 min at 14,000 RPM at 4°C and the protein concentration in the supernatant was determined by the BCA protein assay. Approximately 50 μg of the supernatant was resolved by SDS-polyacrylamide gel electrophoresis (PAGE) and transferred onto PVDF membrane (Bio-rad). The blots were incubated for 1 h in blocking buffer containing 5% nonfat dry milk in Tris-buffered saline (TBS) and then incubated overnight at 4 °C with anti-human NET1 antibody diluted (1:750) in 2% milk in TBS buffer containing 0.1% Tween 20 (TBS-T). After washing with TBS-T, the blots were incubated for 1 h at room temperature with the goat anti-rabbit IgG HRP conjugated secondary antibody (1:2500 dilution) in TBS-T buffer containing 5% milk. The blots were again washed thrice with TBS-T for 10 minutes and then developed with the ECL western blotting detection reagent (GE Healthcare). All blots were re-probed for β-actin (1:10,000) as a loading control. Band intensities of scanned blots were quantified using ImageJ. The integrated intensity of a fixed area was measured, and background levels were subtracted.

Cytotoxicity Studies

The cytotoxicity of MIBG was measured by standard MTT assays in 96-well plates using NB cell lines. After seeding the cells at the desired density and incubating overnight, vehicle control (5% DMSO in PBS) or vorinostat (5 μM) was added to the culture medium. After 24 hours of treatment, the drug-containing medium was replaced with medium containing MIBG at various concentrations and the incubation was continued for additional 72 hours. At the end of the incubation, 20 μL of MTT stock solution (5 mg/mL) was added to each well. After additional incubation for 3 h at 37 °C, the MTT reaction medium was discarded and the purple-blue MTT formazan crystals were dissolved by the addition of 100 μL of 0.1 N HCI in isopropanol. The optical density (OD), which is a measure of the mitochondrial function of the viable cells, was read directly with a microplate reader (model versamax, Molecular Devices Co., CA, USA) at 580 nm and a reference wavelength of 680 nm. Concentration response graphs were generated for each drug using GraphPad Prism software (GraphPad Software, Inc., San Diego, CA, USA). These graphs were analyzed using a curve fit for sigmoid dose-response, and IC_{50} values were derived. Results are expressed as mean IC_{50} values with the standard error of the mean.

Animals

Female CrTac:NCr-Foxn1nu athymic mice (4 to 5 weeks old) were purchased from Taconic (Germantown, NY, USA) and housed under aseptic conditions, which included filtered air, sterilized food, water, bedding, and cages. The experiments on mice were approved by the Institutional Animal Care and Use Committee of University of California at San Francisco. All experimental and animal handling procedures were in accordance with national ethical guidelines.

Preparation of Neuroblastoma Xenografts and Drug Treatment

To study the effect of vorinostat treatment on NET expression *in vivo*, nude mice harboring xenografts of human NB1691 neuroblastoma cells expressing luciferase (NB1691luc) were used. For preparation of NB xenografts, NB1691luc cells were resuspended in serum free RPMI1640 media and 100 μl of this mixture containing 6×10^6 cells were injected in mice by i.v. tail vein injection. Serial tumor measurements were obtained by weekly bioluminescence imaging after an intraperitoneal injection of d-luciferin (Xenogen) at 15 mg/mL in sterile PBS. Twenty-one days after injection of tumor cells, the animals were

divided into vehicle control (5% DMSO in saline) and vorinostat (150 mg/kg i.p.) treated groups (2 per group). Tumors were then harvested from each animal at various time points (1, 3, 6, and 18 hours) after initiation of treatment and lysed with a buffer containing (20 mM Tris HCl pH 7.5–8.0, 150 mM NaCl, 0.5% sodium deoxycolate, 1% Triton X100, 0.1 sodium dodecyl sulfate (SDS), 1 mM EDTA, 1 mM phenylmethylsulphonyl fluoride, and protease inhibitor cocktail). qRT-PCR and Western blot analysis of these tissues was carried out as described under Quantitative Real-Time PCR and Western Blotting section.

In order to study the effect of vorinostat administration on tissue expression of NET in healthy mice not bearing tumors, nude mice (5 per group) were injected with vorinostat (150 mg/kg i.p.) and various tissues were harvested 6 and 18 hours after drug treatment. Each of these tissues was then subjected to total RNA extraction and qRT-PCR analysis as described before.

Biodistribution Measurements of ^{123}I-MIBG

Animals with NB xenografts (described above) were divided into two groups (3 per group) in the following manner: (1) control group = injected with vehicle (5% DMSO in saline i.p.) six hours prior to ^{123}I-MIBG (300 μCi/mouse) by i.v. tail vein injection, (2) treatment group = injected with vorinostat (150 mg/kg i.p.) six hours before i.v. tail vein injection of ^{123}I-MIBG. Two hours after the treatment, the mice were euthanized. Samples of liver, kidney, spleen, heart, and tumor were excised, weighed and their associated radioactivity was measured in an automated Wallac 1480 Wizard gamma counter using the program RiaCalc Wiz (Wallac Oy; Turku, Finland). Blood was also sampled and radioactivity content was normalized to its weight. The uptake of ^{123}I-MIBG was expressed as the fraction of the injected dose per gram of tissue. A correction was made for radioactive decay, which would take place since the time of injection.

Data Analysis—Data were analyzed statistically by unpaired or paired Student *t* tests, as appropriate. Probability values lower than 0.05 were considered statistically significant.

Results

^{123}I-MIBG uptake was increased in hNET transfected cells

Being an analog of monoamine neurotransmitter norepinephrine, the transport of MIBG by NET is well documented.[11] We confirmed the uptake of MIBG by NET in our *in vitro* model using HEK293 cells stably transfected with human NET transporter (HEK-hNET). Due to its ease of handling and shorter half life, we used ^{123}I-labeled MIBG instead of ^{131}I-labeled MIBG in our *in vitro* and *in vivo* studies.[12] The cellular accumulation of ^{123}I-MIBG in HEK-hNET cells [0.484 ± 0.033 μCi/(mg protein-min)] was 13.4-fold higher than in HEK-EV cells [0.036 ± 0.003 μCi/(mg protein-min); $p < 0.0001$; Supporting Information; Fig. S1]. Incubation of ^{123}I-MIBG with a NET inhibitor (desipramine, 10 μM) significantly reduced the cellular accumulation of MIBG in hNET expressing cells (0.042 ± 0.0033 μCi/(mg protein-min); $p < 0.0001$), with no effect in HEK-EV cells (0.030 ± 0.0026 μCi/(mg protein-min); $p > 0.05$).

Neuroblastoma cell lines and tumor samples show high NET expression

Originating from the sympathetic nervous system, neuroblastomas retain the ability of neuronal cells to uptake NE through the neuronal NE transporter. Hence the baseline expression level of NET transcripts in seven NB cell lines and 13 NB tumor samples was examined by qRT-PCR analysis. All the NB cell lines tested showed detectable and variable expression of NET mRNA. The highest expression of NET was observed in LAN5, SK-N-SH and NB1691 cell lines and was in the range of 23–45% of the expression of PGK1 (3-

phosphoglycerate kinase), an abundantly expressed endogenous control (Fig. 1A). NET mRNA was detected in twelve out of thirteen NB tumor samples across a range of expression levels. NET transcripts were expressed at more than 40% of the endogenous control PGK1 in nine out of the 13 tumor samples (Fig. 1B). The comparison of NET transcripts with the endogenous control signifies the high abundance and significance of NET protein to NB cell types.

Vorinostat causes a dose-dependent increase in the levels of expression of NET mRNA and protein in neuroblastoma cell lines

To determine the effect of vorinostat treatment on the expression of NET, we cultured two NB cell lines in the presence of either DMSO (vehicle control) or vorinostat (0.05, 0.10, 0.25, 0.50, 0.75, 1.00, 2.5 and 5.00 μM) for 24 h. The cell lines selected for this purpose (SH-SY-5Y and Kelly) were based on their moderate NET expression and to allow evaluation of *MYCN* amplified (Kelly) and *MYCN* non-amplified (SH-SY-5Y) status of these cell lines. The doses of vorinostat were based on clinically relevant plasma concentrations.[13,14] RT-PCR analysis of mRNA isolated from vorinostat treated cells demonstrated qualitatively a dose-dependent increase in the expression of NET transcripts in both of the cell lines (Fig. 2A).

Using qRT-PCR analysis the increase in NET expression after vorinostat treatment observed earlier was quantified (Fig. 2B). Even the lowest concentration of vorinostat (0.025 μM) resulted in a two-fold increase in NET expression in Kelly cells over the non-treated cells and a maximum increase of 6.7-fold was achieved at 5 μM dose of vorinostat. A dose-dependent increase in NET mRNA expression was also observed in SH-SY-5Y cells after vorinostat treatment with maximum attainable increase of 5.6 fold after exposure to 5 μM concentration of vorinostat. The increase in the expression of NET mRNA observed by RT-PCR and qRT-PCR data, however, does not necessarily prove the presence of functional NET transporter protein. These studies were therefore supplemented with western blotting and functional characterization of elevated NET protein after vorinostat treatment in NB cell lines.

Increases in NET mRNA expression in NB cells after vorinostat treatment were examined for correlations with NET protein levels. NET protein concentrations in Kelly and SH-SY-5Y cells exposed to 1 and 5 μM vorinostat for 24 h were analyzed by Western blot (Fig. 2C). The increase in NET mRNA levels observed in both the NB cell lines was in agreement with the increase in NET protein synthesis. Kelly and SH-SY-5Y cells treated with vorinostat (5 μM) showed approximately 5.3 and 6.9 fold increases in NET protein compared to untreated cells, respectively.

Vorinostat treatment increases uptake of NET substrates *in vitro*

We next performed a functional characterization of NET following vorinostat treatment. The cellular accumulation of a protypical NET substrate, norepinephrine (NE), was determined in the presence and absence of a range of vorinostat concentrations in two NB cell lines (Fig. 3A). The cellular accumulation rate of ^{3}H-NE (15 nM) in NB cells treated for 24 h at the highest vorinostat concentration (5 μM) was 2.5–3.4 fold higher than the corresponding untreated control cells. Specifically, the uptake of ^{3}H-NE in Kelly cells in the presence and absence of vorinostat (5 μM) treatment was 0.252 ± 0.017 nmol/(mg protein–min) and 0.009 ± 0.006 nmol/(mg protein–min), respectively ($P < 0.001$). Similarly, the highest concentration of vorinostat resulted in an accumulation rate of 0.178 ± 0.011 nmol/(mg protein-min) for ^{3}H-NE in SH-SY-5Y cells, which was significantly greater than 0.052 ± 0.004 nmol/(mg protein-min) in untreated cells ($p<0.001$). Both cell lines exhibited a dose-

dependent increase in NE uptake across the range of evaluated vorinostat concentrations (0-5 μM).

Similarly, vorinostat pretreatment (0–5 μM) caused a dose-dependent increase in ^{123}I-MIBG uptake in the NB cells. In the absence of vorinostat treatment, the intracellular concentration of ^{123}I-MIBG after its exposure for 3 minutes to Kelly cells was 0.025 ± 0.001 μCi/(mg protein-min). This intracellular concentration of ^{123}I-MIBG increased 3.9-fold after pretreatment with 5 μM vorinostat (0.097 ± 0.018 μCi/(mg protein-min), $p<0.001$). Similarly, a 2.6-fold enhancement in ^{123}I-MIBG uptake was observed in SH-SY-5Y cells pre-treated with vorinostat (5 μM) (0.062 ± 0.003 μCi/(mg protein-min)) compared to untreated cells (0.024 ± 0.001 μCi/(mg protein-min); $p < 0.001$; Fig. 3B). Furthermore, the increase in cellular uptake of NE and MIBG observed after vorinostat pretreatment was inhibited by desipramine (10 μM), a NET inhibitor (data not shown). When these uptake experiments were performed under various pre-incubation periods or vorinostat (2, 4, 6, 12 and 24 h), the maximum changes in the uptake were observed at the 6-hour time point with a negligible further increase at 24 hours (Supporting Information; Fig. S4), in agreement with maximum increase in NET mRNA and protein observed at that time point (Supporting Information; Fig. S3). The vorinostat pretreatment period of 24 h was selected to capture maximal changes in the uptake of NET substrates and for simplicity of experimentation.

Cytotoxic efficacy of MIBG is enhanced in the presence of vorinostat

To obtain a correlation between vorinostat-induced increases in MIBG uptake in NB cell lines via NET upregulation and the functional consequences of this enhanced uptake on cell growth, we examined the cytotoxicity of MIBG in the presence and absence of vorinostat. The results of standard MTT assays indicate that MIBG in combination with vorinostat is prominently more toxic against all NB cell lines tested when compared to MIBG alone (Table 1). The IC_{50} value of MIBG in the presence of vorinostat is 1.88-3.57 (depending on the NB cell line) order of magnitude lower than its IC_{50} as a single agent. Changes in cell proliferation following exposure to 5 μM vorinostat were less than 10% for 36 hour exposure periods and less than 20% for 48 hours.

Vorinostat treatment caused increases in NET protein levels in neuroblastoma xenografts in mice

The next aim for this study was to obtain *in vivo* proof-of-principle of the observed vorinostat-induced NET upregulation and its functional consequences. Neuroblastoma xenografts created by intravenous tail vein injection of NB1691-luc cells were used for these experiments. After allowing tumors to develop for 21 days, mice were injected with 150 mg/kg of vorinostat or vehicle control intraperitoneally. Tumors harvested at various time points after vorinostat administration were analyzed by Western blotting (Fig. 4A). A 2.1 and 2.5 fold increase in NET protein level compared to the untreated control mice was noticeable at the 1 and 3 h time points respectively, in the vorinostat-treated mice. The tumors at 6 and 18 h time points exhibited 3.8 and 4.2 fold increases in NET protein with vorinostat treatment over the untreated control mice respectively (Supporting Information; Fig. S5A). Similarly, the corresponding changes in NET mRNA expression levels were observed in these samples (Supporting Information; Fig. S5B). The rapid tumor progression observed in this metastatic mouse model and negligible differences in NET expression enhancement prompted us to use the 6 hour time point for biodistribution studies. No change in NET protein expression level was observed in mice treated with the vehicle control over the entire period of the experiment.

The effect of vorinostat on NET transcription was studied in different tissues of healthy mice at 6 and 18 hours following i.p. vorinostat administration (Fig. 4B). The greatest

relative increases in NET mRNA expression levels were in the brain (7.82-fold over untreated control) and in the liver (7.69-fold over untreated control) after six-hours. At the 18 h time point, increases in NET mRNA levels were also observed in the adrenal gland and skin (3.64 and 2.25 fold over untreated controls, respectively).

Biodistribution of ^{123}I-MIBG

The functional effect of increased NET protein level after vorinostat treatment was next evaluated in terms of changes in MIBG *in vivo* biodistribution. Figure 5 presents the biodistribution of ^{123}I-MIBG two hours after intravenous administration in nude mice bearing NB1691-luc human neuroblastoma xenografts. Half of these xenografts received pretreatment with intraperitoneal vorinostat (150 mg/kg) 6 h before MIBG administration. Differences in tissue accumulation due to vorinostat administration reaching statistical significance were observed only in the liver and in tumors. Without vorinostat treatment, the concentration of MIBG in the liver was 0.025 ± 0.003 μCi/(mg tissue-dose injected) whereas with vorinostat pretreatment, the total concentration of MIBG in the liver increased to 0.049 ± 0.006 μCi/(mg tissue-dose injected) ($p < 0.05$; Fig. 5). The greatest increases in MIBG accumulation due to vorinostat treatment were observed in tumors, which were 2.8 fold higher than the corresponding control group [with vorinostat pretreatment: 0.062 ± 0.011 μCi/(mg tissue-dose injected) versus untreated: 0.022 ± 0.003 μCi/(mg tissue-dose injected); $P < 0.05$; Fig. 5]. Although there was a trend toward increase in MIBG concentration after vorinostat pretreatment in other tissues (e.g., kidney, spleen, heart), the difference in concentrations between the vorinostat treated and untreated group did not reach statistical significance. A trend was also observed toward reduced MIBG accumulation in the blood in the vorinostat pretreated group, but the difference did not reach statistical significance [with vorinostat pretreatment: 0.004 ± 0.001 μCi/(mg tissue-dose injected) versus no vorinostat pretreatment: 0.007 ± 0.001 μCi/(mg tissue-dose injected); $P > 0.05$; Fig. 5]. Because the compound does not cross the BBB, MIBG brain accumulation was below the detection limit of the assay.[18]

Discussion

We have demonstrated that exposure to vorinostat at clinically relevant concentrations enhances NET mRNA and protein expression in neuroblastoma cell lines and tumor xenografts. This enhanced NET expression translates into increases in MIBG uptake into model systems, suggesting that the newly synthesized NET protein is functional. While increased MIBG uptake was observed in non-tumor tissues, the greatest vorinostat-induced increase in uptake was in neuroblastoma tumors. This suggests a possible favorable therapeutic index for ^{131}I-MIBG when administered together with vorinostat. We hypothesize that combination of vorinostat and ^{131}I-MIBG will augment intracellular accumulation of ^{131}I-MIBG in patients with neuroblastoma. This hypothesis forms the basis for an ongoing phase 1 clinical trial of this combination in children and young adults with relapsed or refractory neuroblastoma (NANT N2007-03).

Results from our laboratory and others clearly demonstrate that NET is expressed at higher than endogenous levels in almost all NB tumors evaluated (Fig. 1). MIBG, a metabolically stable NE analogue, accumulates in neuroendocrine tissues via NET (Supporting Information; Fig. S1) and MIBG labeled with either ^{131}I or ^{123}I is used for the scintigraphic visualization (diagnosis) and therapy of pheochromocytomas and neuroblastomas.[15,16,17] The polar guanidinium group borne by MIBG precludes its movement across the BBB into the brain,[18] making MIBG highly appropriate for our aim of achieving a high therapeutic index.

The experiments in this study were designed to evaluate the hypothesis that chemically induced upregulation of NET would enhance partitioning of MIBG into NB tumors. The chemical induction of NET expression was inhibition of histone deacetylases (HDAC) through administration of vorinostat. RT-PCR, qRT-PCR and Western blot analysis of NB cells treated with increasing concentrations of vorinostat revealed dose-dependent increases in NET transcription and translation (Fig. 2). The mechanism through which vorinostat upregulates NET expression remains unclear. Vorinostat chelates an essential Zn^{2+} ion, deactivating a host of HDAC isoenzymes. HDAC inhibition causes chromatin opening, making it more accessible to transcription factors and thereby leading to increased expression of cellular proteins. However, due to the intricate secondary interrelationships between cellular transcription factors and cellular proteins, the net result may not necessarily be upregulation of a particular protein. For example, HDAC inhibition may also promote increased acetylation of transcription factors, thereby increasing their activity e.g., in the case of the tumor suppressor p53, HDAC inhibition increases its activity, which in turn may lead to cell cycle arrest and even apoptosis.[19] The pathway through which vorinostat upregulates NET may therefore involve several levels of interplay between transcription factors and chromatin opening. Vorinostat is already approved for the treatment of cutaneous T cell lymphoma (CTCL) and has shown moderate activity as a single agent against neuroblastoma cell lines in preclinical studies.[20] Furthermore a large body of preclinical data also indicates that HDAC inhibitors including vorinostat can act as radiosensitizers across a range of human cancers.[21,22,23,24] Combinations of ^{131}I-MIBG with radiosensitizing agents like topotecan[25] and irinotecan (NANT2004-06) have been successfully evaluated and shown to be tolerable in clinical trials. These results prompted us to evaluate vorinostat/^{131}I-MIBG combination for NB. Vorinostat pretreatment indeed caused increased accumulation of MIBG in NB cells (Fig. 3). The cytotoxicity of MIBG also was vastly enhanced when NB cells were pretreated with vorinostat as opposed to MIBG alone (Table 1). These data conclusively link the increased cellular accumulation of MIBG in the presence of vorinostat with a corresponding increase in its toxicity.

NB tumors are biologically heterogeneous, and may in theory respond dissimilarly to vorinostat exposure. A clinically utilized indicator of NB prognosis is *MYCN* gene amplification and is an indication of advanced disease.[26,27] In order to address some of this heterogeneity, we evaluated two cell lines that differ in their *MYCN* status: the Kelly cell line is *MYCN* amplified while the SH-SY-5Y cell line is not. Throughout the experiments, vorinostat-induced NET upregulation was independent of the *MYCN* status of the cell line. It should, however, be noted that HDAC inhibitors such as valproic acid have been previously shown to downregulate *MYCN*.[28] Indeed, vorinostat was found to downregulate *MYCN* (data not shown) suggesting that any underlying correlation between NET upregulation and *MYCN* status may be masked by the effect of vorinostat on *MYCN*.

The mapping of vorinostat-induced NET overexpression *in vivo* demonstrated increase in NET mRNA transcription in the brain, liver, adrenal gland and skin for a healthy mouse (Fig 4B). This effect was prominent even 6 hours after vorinostat administration. Similar increases in NET protein levels was observed in NB tumors at 6 h time-point (Fig. 4A) which correlated with the significantly increased MIBG uptake in the tumors of vorinostat-treated mice over untreated controls (Fig. 5). Although MIBG uptake also increased in the livers of vorinostat-treated mice, the animal model used in our study contained high degrees of tumor metastasis. The increased MIBG uptake in the liver may possibly have occurred due to the contribution of NB cells metastatic to the liver. ^{131}I-MIBG is associated with a very low-incidence of hepatic toxicity.[29] The current findings nevertheless raise the possibility of increased hepatic toxicity when ^{131}I-MIBG is combined with vorinostat. Clinical trials of the combination will need to monitor for this possibility.

The main dose limiting toxicity of ^{131}I-MIBG is hematologic toxicity. We observed a trend toward decreased plasma concentrations of MIBG in mice treated with vorinostat (Fig. 5). While we were not able to evaluate bone marrow levels of MIBG, it is possible that the combination of vorinostat and ^{131}I-MIBG may result in less hematologic toxicity through two mechanisms. First, if the combination results in increased ^{131}I-MIBG into tumor cells, then a lower dose of ^{131}I-MIBG may be as efficacious as ^{131}I-MIBG given as a single agent at a higher dose. In addition, if bone marrow uptake of ^{131}I-MIBG is reduced by vorinostat treatment though preferential channeling of ^{131}I-MIBG into tumors, then hematologic toxicity may also be reduced.

In spite of many combination therapies tried in the treatment of neuroblastoma, the goal of a very high therapeutic index with sparing of the normal and the developing tissues remains elusive. The strategy designed and developed in this study is perhaps one of the few that are derived specifically from addressing each of the unique aspects of neuroblastoma that differentiate them from other tumors. While the enhancement of MIBG uptake by vorinostat comes about from a biochemical change induced by vorinostat, the sparing of CNS results from biodistribution aspects of MIBG. Through selective partitioning of MIBG into NB tumors by vorinostat administration, it may be possible to achieve desired efficacy from a lower dose of MIBG, potentially mitigating the problematic hematologic toxicity often observed with MIBG therapy.

Supplementary Material

Refer to Web version on PubMed Central for supplementary material.

Acknowledgments

This work was supported by NIH grants GM61390, GM36780, PO1 81403 (KKM) and KL2 RR024130; by a grant (17RT-0126) from the Tobacco-Related Disease Research Program (TRDRP); and by the Alex Lemonade, Dougherty and the Campini Foundation.

Reference

1. Goodman, MT.; Gurney, JG.; Smith, MA.; Olshan, AF. Sympathetic nervous system tumors. In: Ries, LA.; Smith, MA.; Gurney, JG., et al., editors. Cancer Incidence and Survival among Children and Adolescents: United States SEER Program, 1975-1995. National Cancer Institute; Bethesda, MD: 1999. p. 65-72.
2. Maris JM. Recent advances in neuroblastoma. N Engl J Med. 2010; 362:2202–11. [PubMed: 20558371]
3. DuBois SG, Kalika Y, Lukens JN, Brodeur GM, Seeger RC, Atkinson JB, Haase GM, Black CT, Perez C, Shimada H, Gerbing R, Stram DO, Matthay KK. Metastatic sites in stage IV and IVS neuroblastoma correlate with age, tumor biology, and survival. J Pediatr Hematol Oncol. 1999; 21:181–9. [PubMed: 10363850]
4. Takeda N. Simultaneous analyses of monoamines and their metabolites in urine specimens of patients with neuroblastoma. Comp Biochem Physiol C. 1993; 105:373–7. [PubMed: 7900960]
5. Hadrich D, Berthold F, Steckhan E, Bönisch H. Synthesis and characterization of fluorescent ligands for the norepinephrine transporter: potential neuroblastoma imaging agents. J Med Chem. 1999; 42:3101–8. [PubMed: 10447954]
6. Taggart D, Dubois S, Matthay KK. Radiolabeled metaiodobenzylguanidine for imaging and therapy of neuroblastoma. Q J Nucl Med Mol Imaging. 2008; 52:403–18. [PubMed: 19088694]
7. DuBois SG, Matthay KK. Radiolabeled metaiodobenzylguanidine for the treatment of neuroblastoma. Nucl Med Biol. 2008; 35(Suppl 1):S35–48. [PubMed: 18707633]
8. Matthay KK, Yanik G, Messina J, Quach A, Huberty J, Cheng SC, Veatch J, Goldsby R, Brophy P, Kersun LS, Hawkins RA, Maris JM. Phase II study on the effect of disease sites, age, and prior

therapy on response to iodine-131-metaiodobenzylguanidine therapy in refractory neuroblastoma. J Clin Oncol. 2007; 25:1054–60. [PubMed: 17369569]

9. Gediya LK, Chopra P, Purushottamachar P, Maheshwari N, Njar VC. A new simple and high-yield synthesis of suberoylanilide hydroxamic acid and its inhibitory effect alone or in combination with retinoids on proliferation of human prostate cancer cells. J Med Chem. 2005; 48:5047–51. [PubMed: 16033284]
10. Vartak AP, Skoblenick K, Thomas N, Mishra RK, Johnson RL. Allosteric modulation of the dopamine receptor by conformationally constrained type VI beta-turn peptidomimetics of Pro-Leu-Gly-NH_2. J Med Chem. 2007; 50:6725–9. [PubMed: 18052024]
11. Bayer M, Kuçi Z, Schömig E, Gründemann D, Dittmann H, Handgretinger R, Bruchelt G. Uptake of MIBG and catecholamines in noradrenaline- and organic cation transporter-expressing cells: potential use of corticosterone for a preferred uptake in neuroblastoma- and pheochromocytoma cells. Nucl Med Biol. 2009; 36:287–94. [PubMed: 19324274]
12. Mandel SJ, Shankar LK, Benard F, Yamamoto A, Alavi A. Superiority of iodine-123 compared with iodine-131 scanning for thyroid remnants in patients with differentiated thyroid cancer. Clin Nucl Med. 2001; 26:6–9. [PubMed: 11139058]
13. Fouladi M, Park JR, Stewart CF, Gilbertson RJ, Schaiquevich P, Sun J, Reid JM, Ames MM, Speights R, Ingle AM, Zwiebel J, Blaney SM, Adamson PC. Pediatric phase I trial and pharmacokinetic study of vorinostat: a Children's Oncology Group phase I consortium report. J Clin Oncol. 2010; 28:3623–9. [PubMed: 20606092]
14. Kelly WK, O'Connor OA, Krug LM, Chiao JH, Heaney M, Curley T, MacGregore-Cortelli B, Tong W, Secrist JP, Schwartz L, Richardson S, Chu E, Olgac S, Marks PA, Scher H, Richon VM. Phase I study of an oral histone deacetylase inhibitor, suberoylanilide hydroxamic acid, in patients with advanced cancer. J Clin Oncol. 2005; 23:3923–31. [PubMed: 15897550]
15. Shapiro B, Gross MD. Radiochemistry, biochemistry, and kinetics of ^{131}I-metaiodobenzylguanidine (MIBG) and ^{123}I-MIBG: Clinical implications of the use of ^{123}I-MIBG. Med Ped Oncol. 1987; 15:170–7.
16. Hoefnagel CA, Voute PA, DeKraker J, Marcuse HR. Radionuclide diagnosis and therapy of neural crest tumors using iodine-131 metaiodobenzylguanidine. J Nucl Med. 1987; 28:308–14. [PubMed: 3102701]
17. Klingenbiel T, Bader P, Bares R, Beck J, Hero B, Jürgens H, Lang P, Niethammer D, Rath B, Handgretinger R. Treatment of neuroblastoma stage 4 with ^{131}I-meta-iodo-benzylguanidine, high-dose chemotherapy and immunotherapy. A pilot study. Eur J Cancer. 1998; 34:1398–402. [PubMed: 9849423]
18. Gourand F, Mercey G, Ibazizène M, Tirel O, Henry J, Levacher V, Perrio C, Barré L. Chemical delivery system of metaiodobenzylguanidine (MIBG) to the central nervous system. J Med Chem. 2010; 53:1281–7. [PubMed: 20085326]
19. Harms KL, Chen X. Histone deacetylase 2 modulates p53 transciptional activities through regulation of p53-DNA binding activity. Cancer Res. 2007; 67:3145–52. [PubMed: 17409421]
20. De los Santos M, Zambrano A, Aranda A. Combined effects of retinoic acid and histone deacetylase inhibitors on human neuroblastoma SH-SY5Y cells. Mol Cancer Ther. 2007; 6:1425–32. [PubMed: 17431121]
21. Camphausen K, Tofilon PJ. Inhibition of histone deacetylation: a strategy for tumor radiosensitization. J Clin Oncol. 2007; 25:4051–6. [PubMed: 17827453]
22. Chinnaiyan P, Vallabhaneni G, Armstrong E, Huang SM, Harari PM. Modulation of radiation response by histone deacetylase inhibition. Int J Radiat Oncol Biol Phys. 2005; 62:223–9. [PubMed: 15850925]
23. Flatmark K, Nome RV, Folkvord S, Bratland A, Rasmussen H, Ellefsen MS, Fodstad Ø , Ree AH. Radiosensitization of colorectal carcinoma cell lines by histone deacetylase inhibition. Radiat Oncol. 2006; 1:25. [PubMed: 16887021]
24. Munshi A, Tanaka T, Hobbs ML, Tucker SL, Richon VM, Meyn RE. Vorinostat, a histone deacetylase inhibitor, enhances the response of human tumor cells to ionizing radiation through prolongation of gamma-H2AX foci. Mol Cancer Ther. 2006; 5:1967–74. [PubMed: 16928817]

25. Gaze MN, Chang YC, Flux GD, Mairs RJ, Saran FH, Meller ST. Feasibility of dosimetry-based high-dose 131I-meta-iodobenzylguanidine with topotecan as a radiosensitizer in children with metastatic neuroblastoma. Cancer Biother Radiopharm. 2005; 20:195–9. [PubMed: 15869455]

26. Corvi R, Savelyeva L, Schwab M. Patterns of oncogene activation in human neuroblastoma cells. J Neurooncol. 1997; 31:25–31. [PubMed: 9049827]

27. Maris JM, Matthay KK. Molecular biology of neuroblastoma. J Clin Oncol. 1999; 17:2264–79. [PubMed: 10561284]

28. Bell E, Chen L, Liu T, Marshall GM, Lunec J, Tweddle DA. MYCN oncoprotein targets and their therapeutic potential. Cancer Lett. 2010; 293:144–57. [PubMed: 20153925]

29. Quach A, Ji L, Mishra V, Sznewajs A, Veatch J, Huberty J, Franc B, Sposto R, Groshen S, Wei D, Fitzgerald P, Maris JM, Yanik G, Hawkins RA, Villablanca JG, Matthay KK. Thyroid and hepatic function after high-dose ^{131}I-metaiodobenzylguanidine (^{131}I-MIBG) therapy for neuroblastoma. Pediatr Blood Cancer. 2010 ahead of print.

Statement of Translational Relevance

In the preclinical results presented in this report, we validate the rationale of combining a histone deacetylase (HDAC) inhibitor, vorinostat, with the neuroblastoma targeted radiopharmaceutical agent, ^{131}I-metaiodobenzylguanidine (MIBG), for treatment of neuroblastoma (NB). Neuroblastomas are cancers of the sympathetic nervous system that generally retain expression of the norepinephrine transporter (NET). ^{131}I-MIBG, a metabolically stable norepinephrine analog, is a substrate of NET and is in clinical trials for the treatment of NB. We demonstrate in *in vitro* and *in vivo* models that exposure to vorinostat causes increase in NET expression levels in NB tumors and enhanced uptake of ^{123}I-MIBG. The vorinostat-induced increased ^{131}I-MIBG uptake may result in enhanced efficacy of ^{131}I-MIBG against NB. The results of this study provide strong support for co-administration of vorinostat and ^{131}I-MIBG in the treatment of NB. A clinical trial for assessment of this combination in patients with resistant/relapsed neuroblastoma is already underway (NANT N2007-03).

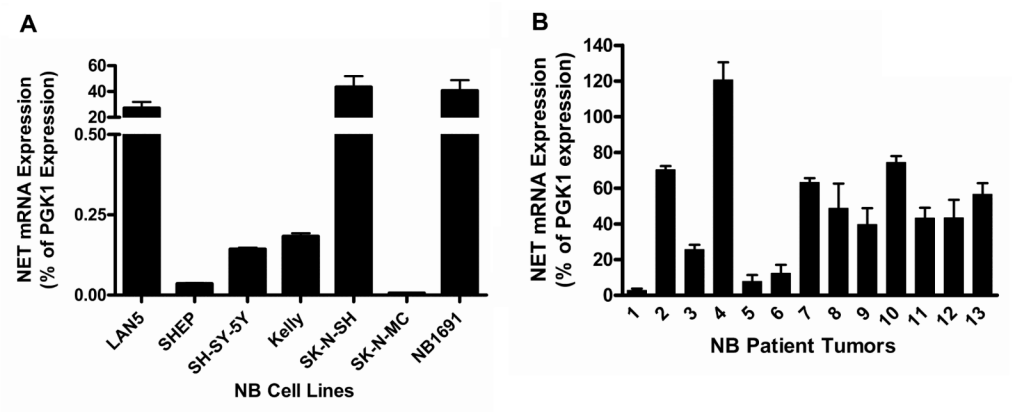

Figure 1.

mRNA expression level of the norepinephrine transporter NET, in neuroblastoma cell lines (A) and tumor samples (B). Total RNA was isolated from seven neuroblastoma cell lines and thirteen neuroblastoma patient tumor samples. The NET mRNA expression was quantified by qRT-PCR as described in Materials and Methods. The data presented is from a single experiment and is reported as the percentage of expression of PGK1, an endogenous control. Similar results were obtained in three independent experiments.

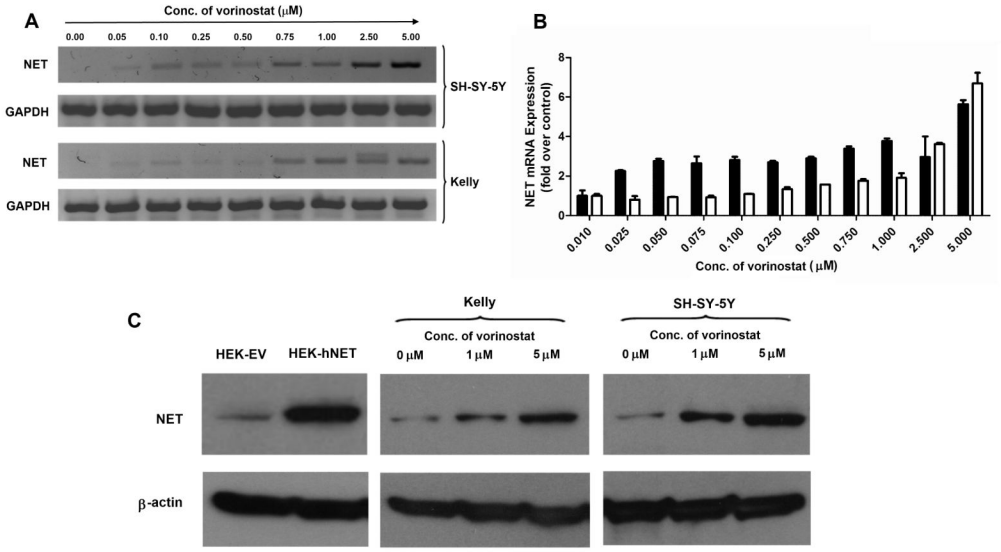

Figure 2.

Enhanced expression levels of NET mRNA in neuroblastoma cell lines treated with vorinostat by RT-PCR (A) and qRT-PCR (B). SH-SY-5Y and Kelly neuroblastoma cells were treated with increasing concentrations of vorinostat ranging from 0 to 5 μM for 24 h, followed by RNA purification and RT-PCR or qRT-PCR using NET-specific primers as described in Materials and Methods. Amplification of GAPDH was used as a loading control for RT-PCR. (C) Enhanced expression of NET protein in neuroblastoma cell lines exposed to vorinostat. Cell extracts from Kelly and SH-SY-5Y cells treated and untreated with vorinostat (1 and 5 μM) for 24 h were prepared and 50 μg of protein lysate from each sample was evaluated by Western blot as described in the Materials and Methods. β-actin was used as a loading control.

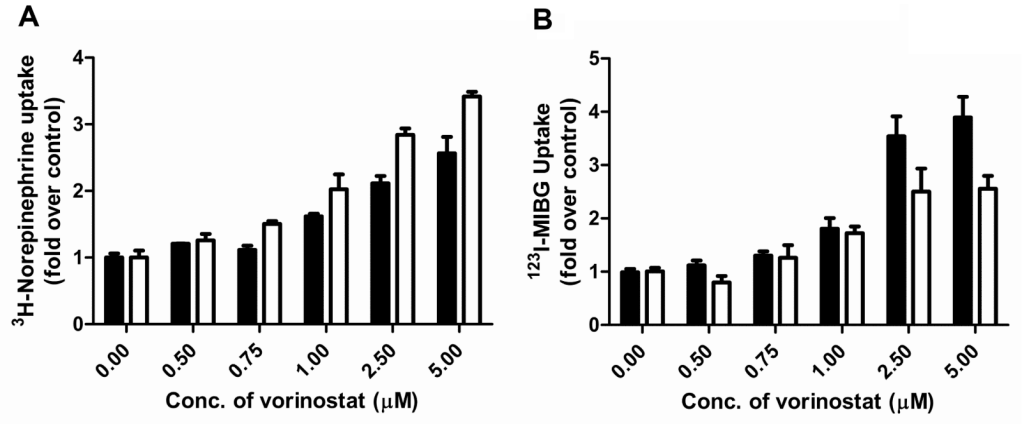

Figure 3.

Increased uptake of ^{3}H-norepinephrine (A) and ^{123}I-MIBG (B) in neuroblastoma cell lines after exposure to vorinostat. Kelly (black bars) and SH-SY-5Y (white bars) cells were exposed to increasing concentrations of vorinostat ranging from 0 to 5 μM for 24 h, followed by uptake of ^{3}H-NE or ^{123}I-MIBG for 3 min. The net uptake is represented as fold over control, where control is the uptake in neuroblastoma cells in the absence of vorinostat pretreatment. Data are expressed as the mean ± SEM from three independent experiments.

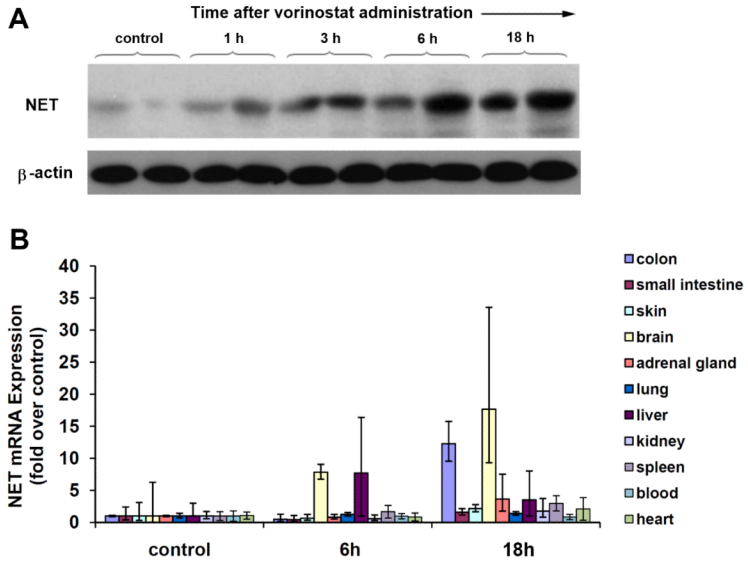

Figure 4.

(A) Enhanced expression of NET protein in neuroblastoma tumors treated with vorinostat *in vivo*. Mice were injected with NB1691-luc cells and after significant tumor development, mice were divided into vehicle control (5% DMSO in saline) and vorinostat treated (150 mg/kg i.p.) groups. Tumors were harvested at 1, 3, 6 and 18 hours after vorinostat treatment and expression of NET protein was determined by Western blot analysis as described in Materials and Methods. (B) Enhanced expression of NET in tissues of healthy Foxn1nu mice 6 and 18 h after intraperitoneal injection of vorinostat (150 mg/kg). Total RNA was isolated from each tissue and quantified for NET mRNA level by qRT-PCR as described in Materials and Methods. Data are represented as the mean ± SEM.

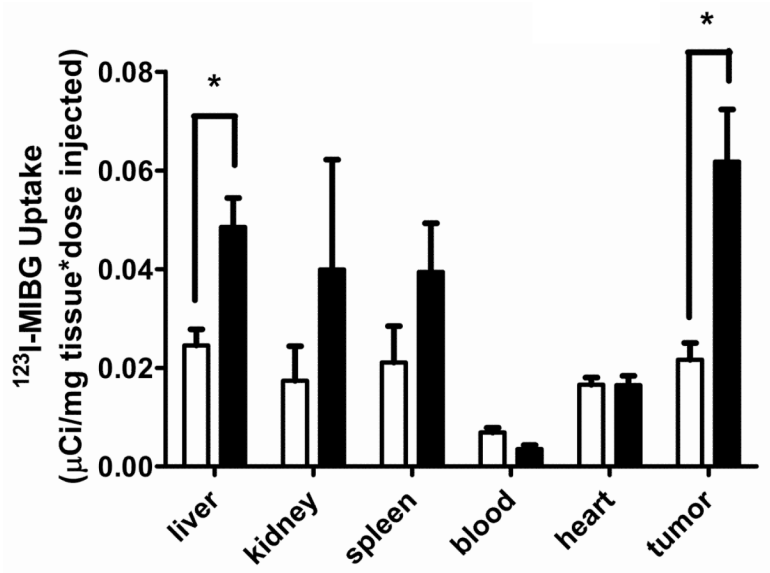

Figure 5.

Biodistribution of ^{123}I-MIBG in Foxn1nu mice after vorinostat treatment. Neuroblastoma xenografts generated by i.v tail vein injection of NB1691-luc cells in mice were treated with vorinostat (150 mg/kg IP; black bars) and vehicle control (5% DMSO in saline; white bars). After 6 h, ^{123}I-MIBG (300 μCi/mouse) was injected by i.v tail vein and tissues were collected after 2 h to measure the accumulation of MIBG as described in Materials and Methods. Data are represented as the mean ± SEM (* $p < 0.05$).”

Table 1

Enhanced efficacy of MIBG in the presence of vorinostat. NB cell lines were pretreated with or without vorinostat (5 μM) for 24 hours before treatment with MIBG for 3 days. Decrease in the IC_{50} of MIBG was observed when vorinostat was present. The enhancement in MIBG efficacy is represented as the resistance factor which is the ratio of IC_{50} of MIBG in the absence and presence of vorinostat. The data are represented as the mean ± SEM of three independent experiments.

	IC_{50} (μM)		
Cell Line	**MIBG**	**MIBG + vorinostat**	**Resistance Factor**
SHEP	70.8 ± 4.51	26.4 ± 2.31	2.68†
Kelly	58.5 ± 3.54	18.3 ± 1.93	3.20†
SH-SY-5Y	52.2 ± 2.24	14.6 ± 1.39	3.57*
SK-N-SH	35.1 ± 5.58	17.4 ± 1.72	2.02‡
NB1691	43.0 ± 5.94	22.9 ± 2.99	1.88‡

*$p < 0.0001$;

†$p < 0.001$;

‡$p < 0.05$